JOURNAL OF MATERIALS SCIENCE 22 (1987) 745–751

An investigation on the bonding of hot-hollow cathode deposited silver layers to type 304 stainless steel

CARL SCHALANSKY, Z. A. MUNIR
Division of Materials Science and Engineering, University of California, Davis, California 95616, USA

D. L. WALMSLEY
Mechanical Engineering Department, Lawrence Livermore National Laboratory, University of California, Livermore, California 94550, USA

The conditions prevailing during the deposition of thick metallic films by the hot-hollow cathode method were investigated. The spacial distribution of temperature, surface roughness, and depth of etch during the pre-deposition etching cycle was investigated for two different sample holder designs. The influence of substrate temperature and the angle of incidence of the vapour on the structure and adhesion of thick silver films to type 304 stainless steel was determined. The nature and strength of adhesion were evaluated on the basis of microscopic examinations and tensile test determinations. Similar evaluations were made on tensile test samples formed through electroplating copper and nickel onto the silver films instead of the joining of two silver-coated samples by hot-isostatic pressing.

1. Introduction

Adhesion and cohesion between solid surfaces are possible as a consequence of the reduction of surface energy accompanying such processes. Bonding between solids, however, will only take place when the distance between the surfaces is sufficiently small (~ 1 nm) so that interatomic forces are effective. The action of such forces, therefore, will be highly dependent on the presence of surface contaminants, e.g. an oxide layer [1]. An analysis of the effect of surface oxide layers on the joining of metallic surfaces has been reported recently [2]. To mitigate, at least in part, the deleterious effect of surface oxides, layers of an intermediate metal are often used in the solid-state bonding of metals [3]. Such layers have been used in the form of thin foils placed between the surfaces to be joined [4], or they may be applied to one or both of the surfaces by electrolytic [5] or vapour phase techniques [6]. In one of the vapour phase deposition methods, the hot-hollow cathode (HHC) technique, a high-current low-voltage arc is utilized to evaporate the coating material and to generate ions of the carrier gas (argon) and the evaporant. These ions are used to clean the substrate prior to depositing the coating material. The HHC process and its use for the deposition of intermediate layers have been adequately described in the literature [7, 8]. Investigations have also been reported on the properties of coatings deposited by this method and on the strength of the resulting bond between the coatings and the substrate [9–12].

The joining of similar and dissimilar metals through the use of the HHC method involves the deposition of thick films of the intermediate layer and the subsequent bonding of the coated surfaces, usually by hot-isostatic pressing (HIP) at relatively low temperatures ensuring the absence of a liquid phase. Interpretations of the structure of thick films deposited by this and by other physical vapour deposition (PVD) methods have been largely based on two proposed models. Movchan and Demchishin [13] proposed a model in which the morphology of the thick deposited films (from micrometers to millimeters) is classified in three structure zones depending on the homologous temperature, T_H, which is defined as the ratio T/T_m, where T_m is the absolute melting temperature of the coating material. Specifically, the model classifies open-porosity columnar structures as belonging to Zone 1 which is favoured at $T_H \leqslant 0.3$. Zone 2, on the other hand, is characterized by densely packed columnar grains. This structure, according to this model [13], exists at $0.3 < T_H < 0.5$. At higher temperatures ($T_H > 0.5$) the structure is characterized by equiaxed grains and is designated as Zone 3 in the model. To account for the effect of the inert gas pressure in sputter deposition processes, Thornton [14] extended the model of Movchan and Demchishin by introducing a transition zone (designating as Zone T) between Zones 1 and 2 of the earlier model. Zone T is characterized by densely packed fibrous grains. According to the Thornton model the inert gas influences the structure of the deposited layer through modification of the energy of the condensate atoms in sputter deposition processes.

According to the two models described above [13, 14], the dependence of the film structure on

0022–2461/87 $03.00 + .12

temperature is primarily the consequence of changes in diffusional fluxes of condensate atoms. At low temperatures, those corresponding to Zone 1, surface diffusion fluxes are relatively limited leading to growth of the condensate nuclei in a perpendicular direction to the substrate, i.e. the opposite direction to the maximum heat flow. Lack of significant surface diffusion fluxes of condensate atoms on the substrate is proposed as the explanation for the observed open-porosity columnar structure of Zone 1. Higher substrate surface roughness and an oblique angle of incidence of the vapour favour the occurrence of Zone 1 structure [15]. As the temperature is increased, surface diffusion contribution becomes dominant and Zone 2 structures prevail. At still higher temperatures, volume diffusion becomes significant and Zone 3 structures prevail [15–17].

In this paper we report the results of an investigation of the prevailing conditions during the HHC deposition of thick silver films on type 304 stainless steel substrates, and on the effect of these conditions on the structure and adhesion of these films.

2. Experimental materials and methods

The HHC assembly consisted of a 0.24 cm thick, 0.8 cm o.d. tantalum tube which served as the cathode, and a 5 cm diameter tantalum crucible (maintained at ground potential) which served as a reservoir for the evaporant. d.c. power supplies are used to provide an initial, −2000 V, bias to the tantalum (cathode) tube. Under high vacuum conditions no discharge takes place but as argon gas is allowed to flow at 46 atm $cm^3 min^{-1}$ through the cathode, the chamber pressure rises to 0.7 Pa and an electric discharge is initiated. Ions created in the discharge bombard the cathode causing it to heat up to temperatures where thermionically-generated electrons are emitted. During this transition a d.c. arc welding power supply is switched on to supply the needed current and the cathode bias is turned off. The ions are directed by means of an electromagnet to the crucible holding the metal to be evaporated, in this case silver. The HHC process produces high concentrations of ions: argon ions from the arc discharge and evaporant ions resulting from the interaction of electrons with the evaporant atoms. These ions are directed towards the substrate through the biasing of the latter at −2000 V, thus, causing the etching of the substrate. The etching cycle is followed by the coating cycle during which the bias of the substrate is removed. Additional details of the HHC method appear in previous publications [7, 8].

Substrates, made from type 304 stainless steel, were in the form of cylinders with approximate diameter and height of 15.3 and 7.9 mm, respectively. These cylinders were inserted into closely machined holes in a 32 cm diameter, 8.0 mm thick plate of stainless steel. This design configuration made it possible to investigate accurately the thermal and spacial characteristics of the HHC process. Substrates were positioned radially in the substrate holder to make possible the determination of the effects of temperature and the angle of incidence of the vapour. For the geometric configuration used in this work the angle of the incidence varied from 0 to 7° for the centre of the substrate holder to 32 to 42° for the edge of this plate. The existence of a range of angles for each location is consequence of the relatively large diameter of the crucible holding the silver charge. The temperatures of the substrate cylinders were monitored by thermocouples inserted in holes drilled in the substrate holder plate close to the cylinders. Prior calibration runs have shown that the differences between the readings of these thermocouples and those placed in contact with the surfaces of corresponding substrates were within 4%.

To obtain coatings at different temperatures, stainless steel spacers and a copper conduction plate were used between the substrate holder and a rotatable water-cooled plate. As will be discussed in a subsequent section, the former configurations provided generally higher coating temperatures with a strong dependence on the radial distance and the latter configurations gave lower but uniform temperatures across the substrate holder. Prior to their insertion into the substrate holder, substrate cylinders were lapped with SiC using five successively finer grit ending with 600. Following the final polishing operation, each substrate was degreased in trichloroethane and stored in sealed plastic bags until used in the coating experiments. Storage time varied between 7 and 10 days. Substrate samples placed near the centre of the holder were randomly oriented with respect to the polishing scratches, while those placed near the outside edge of the holder were oriented such that their polishing scratches were in a tangential direction. Following the positioning of the substrates, the tantalum crucible is cleaned and charged with typically 42 to 63 g of high purity silver, and the system is evacuated to a pressure of 100 μPa or lower. Following an ion etching cycle (during which the substrate holder is negatively biased), silver is deposited onto the substrate to a thickness of 25 μm for samples placed near the centre of the holder. All coated substrates were allowed to cool in vacuum to a minimum of 70° C before exposure to the atmosphere.

In order to assess the strength of the bond between the silver films and the 304 stainless steel substrates, tensile test samples were made using two distinctly different approaches. One of the approaches involved the hot-isostatic pressing (HIP) of two coated samples and the subsequent machining of a tensile test specimen from the bonded couple. HIP bonding was carried out in evacuated cans subjected to a temperature of 600° C and an external pressure of 200 MPa. In the other method of forming tensile test samples, nickel or copper were electroplated onto the silver coating to provide adequate geometries from which to machine the tensile test samples. The tensile test samples were of the conical-head design, with a gauge length and diameter of 6.6 and 5.3 mm, respectively. The aspect ratio (ratio of diameter to length) of these specimens was larger than that recommended by ASTM. Larger aspect ratios can lead to non-uniform stress distribution. To assess this potential shortcoming of the tensile specimen, two unbonded specimens (i.e. made

from one bar) were machined from stainless steel stock material. One of the specimens was drilled axially to remove approximately one-half of the stress area so as to eliminate the low-stress central core. The other sample was tested without further modification. Both specimens were tensile tested, each with three strain gauges positioned 120° around its circumference. At a given stress, the difference in the observed surface strains between the two specimens is an indication of a stress concentration at the outer regions. These experiments showed that the specimen geometry used in this study had near-surface stresses which were 25% higher than the stresses near the core.

3. Results and discussion

3.1. Thermal and spacial characterization of the HHC process

The temperature of a substrate holder plate during a complete cycle in the HHC process is shown in Fig. 1 where the temperature is plotted as a function of time in the etching and coating stages. The plate was fastened by a collet to the rotating fixture and thus, was cooled at its edge. Temperatures were measured at three locations: the centre of the plate, the edge of the plate, and an intermediate position (4.45 cm from the centre of the 21 cm diameter plate). As seen from Fig. 1, the temperature during the etching cycle is not constant, regardless of the location of measurement. In contrast, the temperature during the coating cycle is relatively constant and showed a dependence on the radial distance. In order to determine the effect of temperature and radial position on the depth of etch we devised two experimental arrangements such that under one configuration we have a radial temperature gradient on the plate and under the second configuration we are able to maintain a constant temperature profile across the plate. The results for the first configuration are shown in Fig. 2. Each of the curves shown in this figure represents the radial distribution of temperature for the indicated duration of etching.

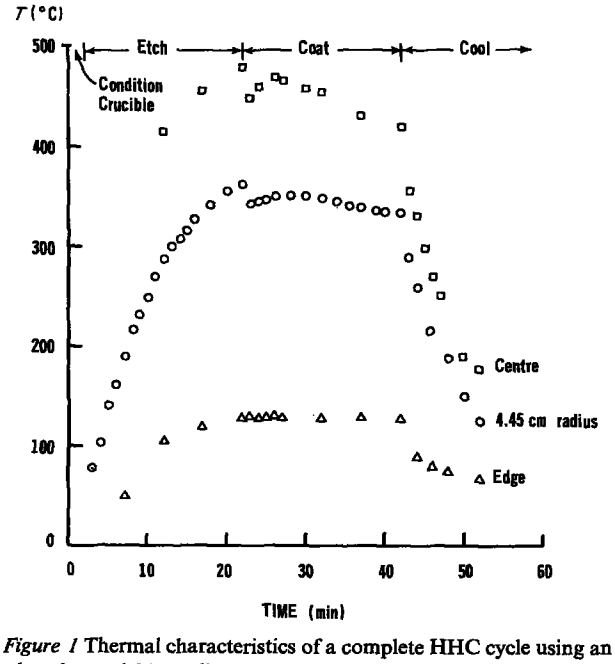

Figure 1 Thermal characteristics of a complete HHC cycle using an edge-clamped 21 cm diameter stainless steel substrate.

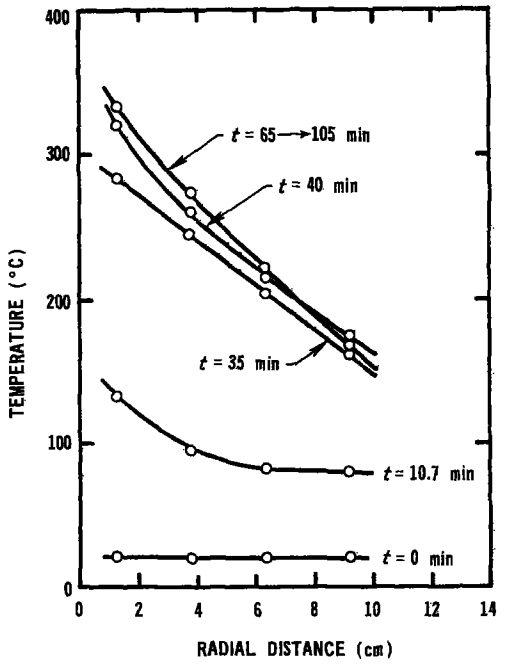

Figure 2 The radial distribution of the temperature of a stainless steel substrate ion-etched for various times.

At any given position along the radius, the temperature increases with increasing etching time up to 65 min. Longer etching times (up to 105 min) had no effect on the value and radial distribution of the temperature. Depth of etch of the substrate resulting from a 105 min long etching cycle is shown in Fig. 3 plotted as a function of radial distance. Also plotted in Fig. 3 are the results of surface roughness measurements on etched surfaces. The depth of etch decreased with increasing radial distance and decreasing temperature. However, as will be shown later, it is the former that is the determining factor on the depth of etch distribution. The data for the roughness of the etched surfaces exhibited a maximum at a location approximately

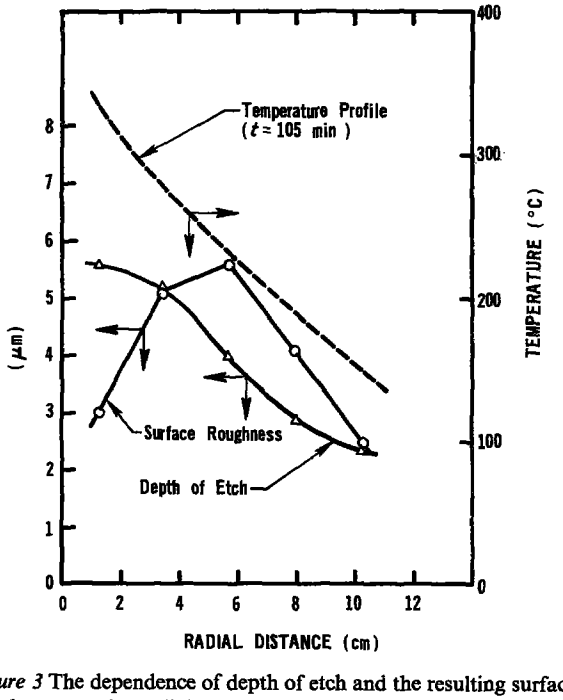

Figure 3 The dependence of depth of etch and the resulting surface roughness on the radial distance for a non-uniform temperature distribution.

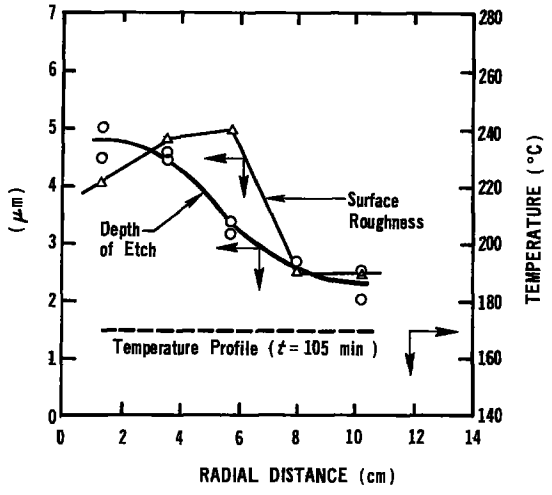

Figure 4 The dependence of depth of etch and the resulting surface roughness on the radial distance for a uniform temperature distribution.

midway between the centre and edge of the plate. The lack of correlation between the depth of etch and the roughness of the etched surface is puzzling and remains unexplained.

In the second experimental configuration where the temperature was maintained constant across the entire plate, the depth of etch showed a strong dependence on the radial distance as shown in Fig. 4. The reproducibility of the depth of etch is indicated by the reasonable agreement between two typical runs shown in Fig. 4. Also shown in this figure is the dependence of the roughness on the radial distance of surfaces etched for 105 min under a constant and uniform temperature of approximately 170° C, as shown in the figure. Analogous to the results reported Fig. 3, the roughness results for a constant temperature configuration showed a maximum at a point about halfway between the centre and the edge of the plate.

A comparison of the depth of etch data on Figs 3 and 4, lead to the conclusion that this experimental parameter is governed primarily by the radial distance. The depth of etch curve for a constant temperature profile is basically the same as that obtained when a temperature gradient of about 180° C existed during the etching stage.

3.2. Bond strength and morphology

Results from ultimate tensile strength testing are shown in Table I. With the exception of the results obtained from HIP-bonded specimens coated at 530° C with zero angle of incidence, the data listed in Table I are fairly uniform and provide the following general conclusions:

TABLE I Bond breaking strength of electroformed and HIP-bonded specimens

Coating temperature (°C)	Angle of incidence (deg)	Mean Breaking Strength (MPa)	
		EP*	HIP*
120	0	381	394
	37.3	382	407
530	0	437	336
	37.3	405	420

*EP and HIP refer to electroplated and HIP-bonded specimens, respectively.

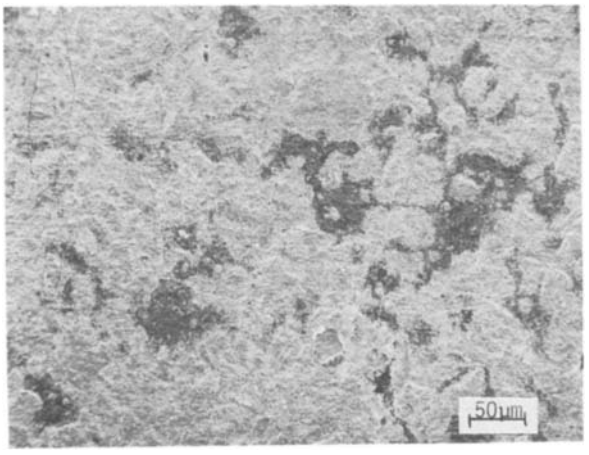

Figure 5 Unbonded (dark) areas indicative of failure at the silver–silver interface.

1. For any given condition, the results indicate that electroplated and HIP-bonded joints have approximately the same strength.
2. Variation of the angle of incidence of the vapour, θ, from zero to 37° resulted in a small and probably insignificant difference in the breaking strength of the specimens.
3. With the exception noted above, the results show that specimens coated at the higher temperature are somewhat stronger than their counterparts coated at the lower temperature. However, the magnitude of the increase in the breaking strength is relatively small, not exceeding 15% in any case. These results further imply that Zone T and 2 structures have similar strengths when bonded to stainless steel.
4. For the electroformed specimens the results show that the use of nickel or copper gives the same breaking strength, within the experimental uncertainty.

The low strength of the high temperature coated and HIP-bonded samples is apparently the consequence of poor bonding between the coated surfaces. Examination of the fracture surfaces from one of these samples showed evidence of failure at the silver–silver interface. Fig. 5 shows large unbonded (dark) areas on the fracture surface. Examination of these areas at a higher magnification shows the absence of features suggestive of ductile failure similar to that seen in the regions surrounding the dark areas (see Figs 6a and b). These features were nearly identical on both sides of the fracture plane. There was no evidence of failure at or near the silver–stainless steel interface. Examined fracture surfaces of all other HIP-bonded samples showed little if any failure at the silver–silver interface. Typically, these samples failed at or near the silver–stainless steel interface.

Fig. 7 shows the stainless steel side of a failed nickel-electroplated specimen. Large areas of silver which had been separated from the nickel interface are evident as well as regions showing failure in the silver layer near the silver–stainless steel interface. The

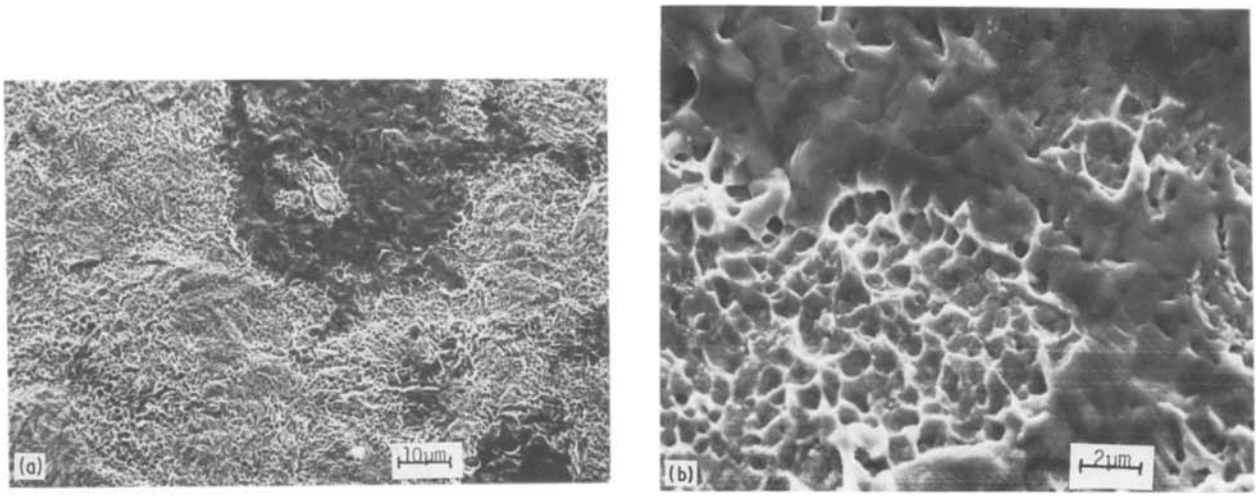

Figure 6 (a, b) The absence of evidence of ductile failure in unbonded (dark) regions. Compare to surrounding areas.

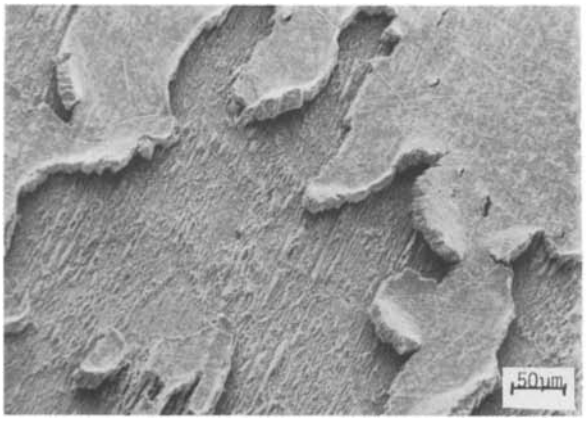

Figure 7 The stainless steel side of a failed nickel-plated specimen.

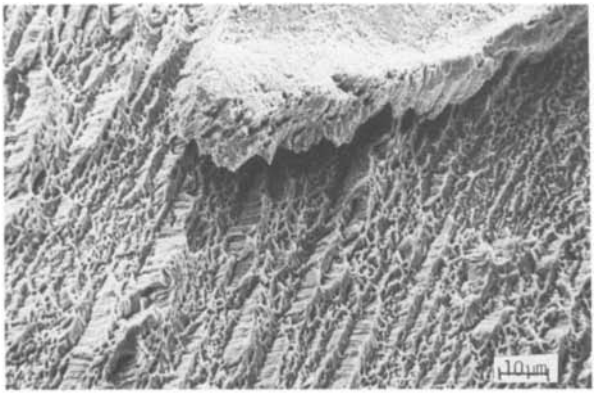

Figure 8 Evidence of ductile failure in the silver layer near the stainless steel–silver interface.

scratch marks on the top of the silver layer were produced through a preparation step prior to the electrodeposition of nickel. A closer (higher magnification) examination of this surface reveals a typical ductile fracture of the silver. The generally parallel pattern of the fracture (Fig. 8) is indicative of the polishing process on the underlying stainless steel substrate. Examination for the other side of this fracture plane, i.e. the nickel side shows a large percentage of failure at the silver–nickel interface; see Figs 9a and b.

Figs 10a and b show the fracture surfaces of a specimen which was formed by the HIP-bonding of two stainless steel surfaces coated with silver at 120° C with $\theta = 37°$. Failure appears to take place in the silver layer near the silver–stainless interfaces.

3.3. Film structure dependence on the angle of incidence of the vapour

Examination of the microstructure of sectioned silver coatings on stainless steel substrates revealed, as expected, the dependence of the orientation of the grains on the angle of incidence of the vapour.

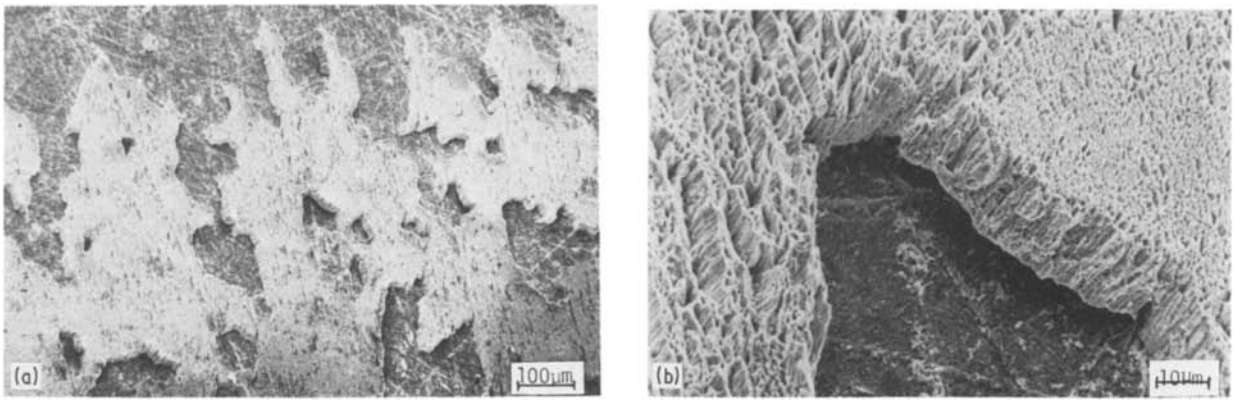

Figure 9 (a, b) Evidence of failure at the nickel–silver interface for nickel-plated specimens.

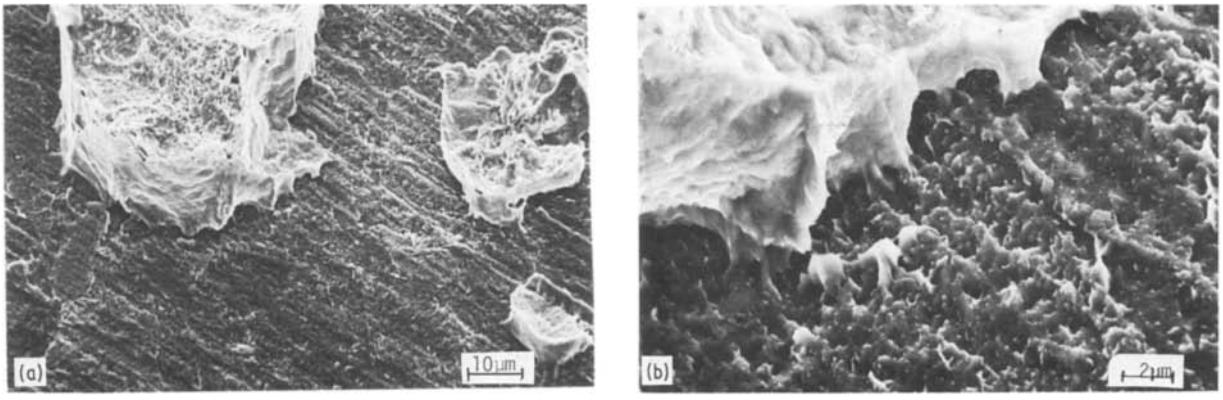

Figure 10 (a, b) Fracture surface of a HIP-bonded stainless steel specimen coated at 120° C with $\theta = 37°$.

However, this dependence was observed only when the vapours were deposited on relatively cool (120° C) substrates. Fig. 11 shows the structure of the grains and their orientation relative to the substrate for a silver coating deposited at $\theta = 0°$ on a stainless steel substrate held at 120° C. In contrast, Fig. 12 shows the microstructure of a silver coating deposited under otherwise identical conditions except for θ being 37°. The correlation between the direction of growth of the silver grains and the angle of incidence of the vapour was not observed for coatings deposited at substrates held at 530° C. Figs 13 and 14 show the microstructures of such coatings deposited under conditions of θ being zero and 37°, respectively.

Regardless of their orientation, silver grains grown at the higher temperatures (530° C) are distinctly different in morphology from those grown at the lower temperature (120° C). Grains grown on cooler substrates are more fibrous in appearance and are suggestive of morphologies ascribed on Zone T in the

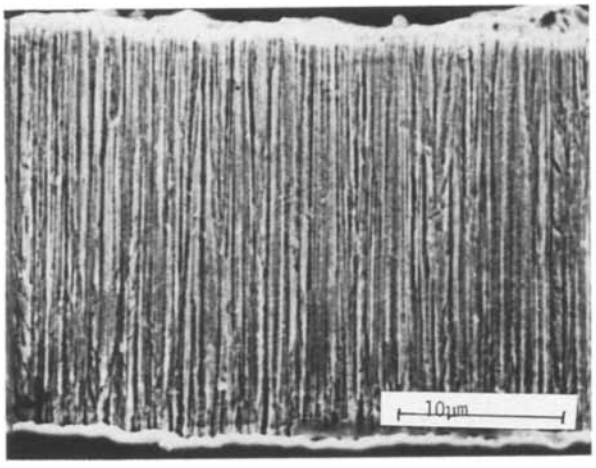

Figure 11 Orientation and structure of a silver film grown on a low temperature (120° C) substrate with a normal angle of incidence of the vapours ($\theta = 0°$).

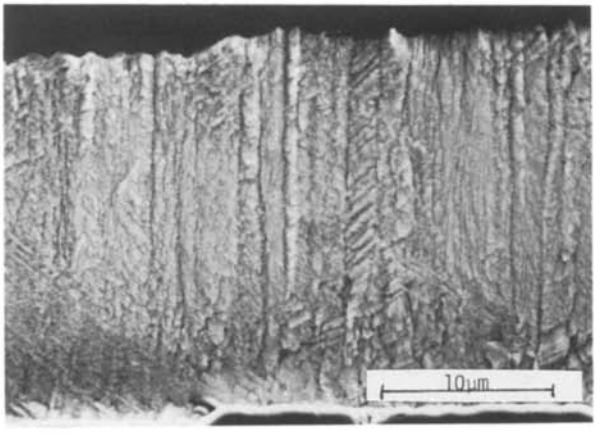

Figure 13 Orientation and structure of a silver film grown on a high temperature (530° C) substrate with a normal angle of incidence of the vapours ($\theta = 0°$ C).

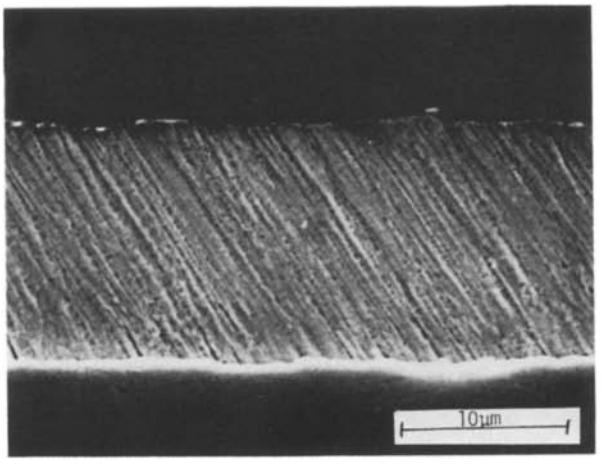

Figure 12 Orientation and structure of a silver film grown on a low temperature (120° C) substrate with an oblique angle of incidence of the vapours ($\theta = 37°$).

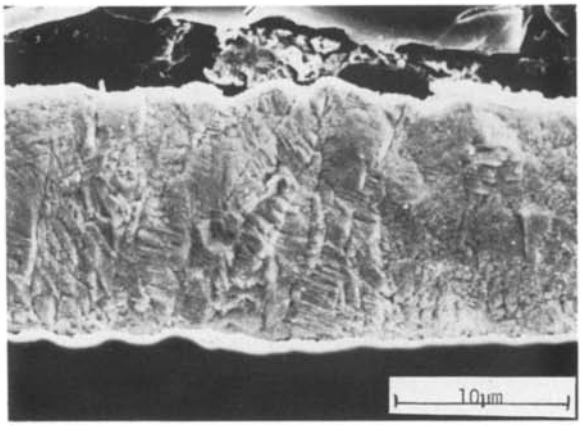

Figure 14 Orientation and structure of a silver film grown on a high temperature (530° C) substrate with an oblique angle of incidence of the vapours ($\theta = 37°$ C).

Thornton model [14]. A substrate temperature of 120° C gives a homologous temperature T_H of 0.32 for silver. According to the Thornton model, Zone T is predicated for this value of T_H and the condensate is expected to be made up of densely packed fibrous grains. For films grown at the higher temperature (530° C), the model predicates a Zone 2 structure having a columnar structure. The present findings are in agreement with this prediction as seen in Figs 13 and 14.

Microhardness measurements were made on coatings deposited at the low (120° C) and high (530° C) temperatures. The average values resulting from such measurements are 161 and 137 (15 g Knoop hardness) for the low and high temperatures, respectively. The decrease in hardness with increase in the substrate temperature is in qualitative agreement with the observations of Movchan and Demchishin [13].

Acknowledgements

This work was supported by a grant from the Lawrence Livermore National Laboratory. We are grateful for the support and assistance of Joe Arluck and Hal Whitlow throughout the course of this research.

References

1. J. L. JELLISON, in "Surface Contamination: Genesis, Detection, and Control", Vol. 2, edited by K. L. Mittal (Plenum Press, New York, 1979) p. 899.
2. Z. A. MUNIR, *Welding J. (Res. Suppl.)* **62** (1983) 333-s.
3. J. L. KNOWLES and T. H. HAZLETT, *ibid.* **49** (1970) 301-s.
4. D. HAUSER, P. A. KRAMER and J. H. DEDRICK, *ibid.* **46** (1967) 11-s.
5. C. H. CRANE, D. Y. LOVELL, W. A. BAGINSKI and M. G. OLSEN, *ibid.* **46** (1967) 23-s.
6. M. O'BRIEN, C. R. RICE and D. L. OLSEN, *Weld. J.* **55** (1976) 25.
7. J. R. MORLEY and H. R. SMITH, *J. Vac. Sci. Technol.* **9** (1972) 1377.
8. D. G. WILLIAMS, *ibid.* **11** (1974) 374.
9. G. MAH, P. S. MCLEOD and D. G. WILLIAMS, *ibid.* **11** (1974) 663.
10. P. S. MCLEOD and G. MAH, *ibid.* **11** (1974) 119.
11. P. D. CALDERSON, D. R. WALMSLEY and Z. A. MUNIR, *Welding J. (Res. Suppl.)* **64** (1984) 104-s.
12. R. S. ROSEN, D. R. WALMSLEY and Z. A. MUNIR, *ibid.* **65** (1986) 83-s.
13. B. A. MOVCHAN and A. V. DEMCHISHIN, *Phys. Met. Metallog.* **28** (1969) 83.
14. J. A. THORNTON, *J. Vac. Sci. Technol.* **11** (1974) 666.
15. S. CRAIG and G. L. HARDING, *ibid.* **19** (1981) 205.
16. J. A. THORNTON, *Ann. Rev. Mater. Sci.* **7** (1977) 239.
17. R. F. BUNSHAH and R. S. JUNTZ, *J. Vac. Sci. Technol.* **9** (1972) 1404.

Received 4 April
and accepted 30 June 1986